

# 508. Investigation of contact point trajectories of the beam type piezoelectric actuator with two preloaded masses

D. Mazeika<sup>1a</sup>, R. Bansevicius<sup>2b</sup>, G. Kulvietis<sup>1c</sup>

<sup>1</sup> Vilnius Gediminas Technical University, Sauletekio al. 11, LT-10223 Vilnius, Lithuania,

<sup>2</sup> Kaunas University of Technology, Kestucio st. 27, LT-44312 Kaunas, Lithuania

**E-mail:** <sup>a</sup>*Dalius.Mazeika@fm.vgtu.lt*, <sup>b</sup>*Ramutis.Bansevicus@ktu.lt*, <sup>c</sup>*Genadijus.Kulvietis@fm.vgtu.lt*

*(Received 09 September 2009; accepted 27 November 2009)*

**Abstract.** The results of numerical modeling and simulation of beam type piezoelectric actuator with two additional masses are given in the paper. Multimode oscillations of the actuator and trajectory of contact point motion strongly depend on location and weight of the additional masses so the aim of the paper was to investigate the dependencies between these parameters under harmonic excitation. Operation principle of the actuator is based on multimode resonant vibrations where superposition of longitudinal and bending modes is used. Two different excitation schemes of electrodes are used to achieve direct and reverse motion of the slider. Numerical study of the trajectories was performed using the finite element method. Dominating coefficients of the oscillations were employed to identify particular modal shapes of the actuator. Dependences between parameters of contact point trajectories and the weight and location of additional masses were determined and analyzed.

**Keywords:** piezoelectric actuator, beam with additional masses, trajectories of contact point

## Introduction

Piezoelectric actuators are widely used for high precision mechanical systems such as positioning devices, manipulating systems, control equipment and etc [1]. Piezoelectric actuators have advanced features such as high resolution, short response time, compact size, and good controllability [1, 2]. Many design principles of piezoelectric actuators are proposed and used [3]. Summarizing its all the following types of piezoelectric actuators can be specified: traveling wave, standing wave, hybrid transducer, and multimode vibrations actuators [2, 4].

Beam type piezoelectric actuator of multimode vibrations is analyzed in the paper. Two basic design approaches of beam type actuator are used to achieve elliptical trajectory of contact point. The first approach is to determine specific pattern of the electrodes for excitation and the second is to find particular geometrical parameters of the beam when resonant frequencies of two vibration modes coincide [3]. A new design principle how to excite multimode vibrations of the beam type piezoelectric actuator is proposed i. e. multimode vibrations of the beam type actuator can be achieved by adding external mass element. Advantage of this design principle is that elliptical trajectories of the contact point can be obtain at resonant frequency without changing geometry of the actuator or pattern of the electrodes. Numerical modeling of piezoelectric actuator was carried out to evaluate operating principle and to investigate dependences between parameters of contact point elliptical trajectories and the weight values and location of additional masses

## Operating principle of piezoelectric actuator

Configuration of actuator includes bulk type piezoceramic beam and two steel masses that are glued at the top surface of the beam (Fig. 1). Polarization vector of piezoceramic is oriented along thickness of the beam and piezoelectric effect  $d_{31}$  is used for the actuation. Electrodes are located at the bottom of the beam and are divided into two equal sections (Fig. 1). This pattern of electrodes is used to realize two different excitation schemes and to obtain direct and reverse motion of the slider.

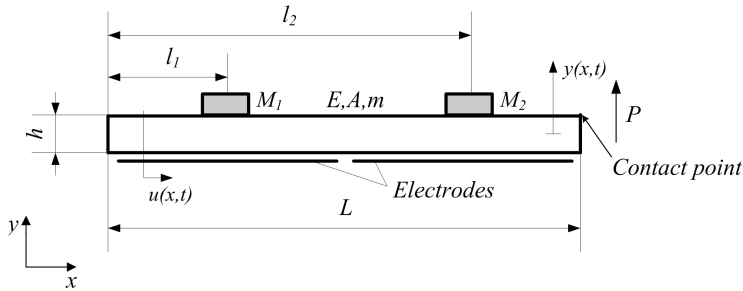


**Fig. 1.** Model of beam type piezoelectric actuator with two additional masses

Operating principle of the actuator is based on using longitudinal and bending multimode resonant vibrations. Two different resonant frequencies are used for actuation. Superposition of the 1<sup>st</sup> longitudinal mode and the nearest bending mode is used to obtain elliptical trajectory of contact point and to achieve direct motion of the slider. Excitation scheme when voltage with the same phase is applied on the both electrodes is used for this case (Fig. 1). Superposition of the 2<sup>nd</sup> longitudinal mode and the nearest bending mode is used to obtain reverse motion of the slider. Excitation voltage has phase difference by  $\pi$  on different electrodes in this case (Fig. 1). Bending mode number participating in superposition depends on  $h/l$  ratio of the piezoceramic beam.

## Equations of motions

The governing differential equation of longitudinal vibrations of the beam type piezoelectric actuator with additional masses  $M_1$  and  $M_2$  can be written as follows [5, 6, 7]:

$$m(x) \frac{\partial^2 u(x,t)}{\partial t^2} - \frac{\partial}{\partial x} \left( EA \frac{\partial u(x,t)}{\partial x} \right) + C_l(x,t) = F_{piez}(t) \quad (1)$$

where  $u(x, t)$  denotes the axial displacement at point  $x$  and time  $t$ ,  $m$  is mass of the beam type actuator,  $E$  is elastic modulus of piezoceramics,  $A$  is cross-section area of beam,  $C_l$  is damping function, and  $F_{piez}$  is mechanical force obtained due to inverse piezoelectric effect  $d_{13}$ .  $F_{piez}$  can be calculated using following equation:

$$F_{piez}(t) = Ube_{31} \sin \Omega t \quad (2)$$

where  $U$  is amplitude of excitation voltage,  $b$  is the width of beam and  $e_{31}$  is piezoelectric coefficient,  $\Omega$  is excitation frequency of the electrodes. Lets denote the axial displacements in

the regions to the left of mass  $M_1$  as  $u_1(x, t)$ , between  $M_1$  and  $M_2$  as  $u_2(x, t)$  and to the right of  $M_2$  as  $u_3(x, t)$  where all these displacements are subject to the Eq. 1. Since the analyzed beam is unsupported beam, only matching conditions are defined:

$$\begin{aligned} u_1(l_1, t) &= u_2(l_1, t); \quad u_2(l_2, t) = u_3(l_2, t) \\ EAu_1'(l_1, t) - EAu_2'(l_1, t) + M_1\ddot{u}(l_1, t) &= 0 \\ EAu_2'(l_2, t) - EAu_3'(l_2, t) + M_2\ddot{u}(l_2, t) &= 0 \end{aligned} \quad (3)$$

Bending vibrations are obtained in the actuator as well when  $F_{piez}$  is applied. Differential equation of bending vibrations can be written as [6, 8]:

$$m(x) \frac{\partial^2 y(x, t)}{\partial t^2} + \frac{\partial^2}{\partial x^2} \left( EI \frac{\partial^2 y(x, t)}{\partial x^2} \right) + C_f(x, t) = F_{piez} \frac{\partial^2 y(x, t)}{\partial x^2} \quad (4)$$

where  $y(x, t)$  is transversal displacement,  $I$  is inertia moment of cross-section of the beam,  $C_f$  is damping function. Corresponding matching conditions for the bending vibrations are defined as follows:

$$\begin{aligned} y_1(l_1, t) &= y_2(l_1, t); \quad y_2(l_2, t) = y_3(l_2, t) \\ EIy_1''(l_1, t) + EIy_2''(l_1, t) - M_1\ddot{y}(l_1, t) &= 0 \\ EIy_2''(l_2, t) + EIy_3''(l_2, t) - M_2\ddot{y}(l_2, t) &= 0 \end{aligned} \quad (5)$$

Solution of Eq. 1 and Eq. 4 defines the trajectory of contact point movement and can be written in the following form [6]:

$$u(x, t) = \sum_{n=1}^{\infty} e^{-\alpha_n t} [G_n(x) T_n(\bar{\omega}_n, t)] \quad (6)$$

$$y(x, t) = \sum_{n=1}^{\infty} [e^{-\alpha_n t} H(\bar{\omega}_n, t) + Y_n(\bar{\omega}_n, \alpha_n, t)] y_n(x) \quad (7)$$

here

$$\left. \begin{aligned} H(\bar{\omega}_n, t) &= (A_n \sin \bar{\omega}_n t + B_n \cos \bar{\omega}_n t) \\ \bar{\omega}_n &= \sqrt{\omega_n^2 - \alpha_n^2} \end{aligned} \right\} \quad (8)$$

where  $G_n$  and  $T_n$  are harmonic functions,  $A_n$  and  $B_n$  are coefficients, obtained from initial conditions and  $Y(\bar{\omega}_n, \alpha_n, t)$  is integral function,  $y_n(x)$  is the modal shape of bending vibrations and  $\alpha$  is damping coefficient. Referring to the Eq. 6 and Eq. 7, vibrations of the actuator depend on the additional mass and its location on the actuator. However, only single component of vibrations is calculated using Eq. 6 and Eq. 7. In order to analyze multimode vibrations of the actuator, it is convenient to apply finite element method. Then equation of motion of piezoelectric actuator with additional masses can be written as follows [9]:

$$\left. \begin{aligned} [M] \{\ddot{u}\} + [C] \{\dot{u}\} + [K] \{u\} + [T] \{\varphi\} &= \{F\} \\ [T]^T \{u\} - [S] \{\varphi\} &= \{Q\} \end{aligned} \right\} \quad (9)$$

where  $[M]$ ,  $[K]$ ,  $[T]$ ,  $[S]$ ,  $[C]$  are accordingly matrices of mass, stiffness, electro elasticity, capacity, damping;  $\{u\}$ ,  $\{\varphi\}$ ,  $\{F\}$ ,  $\{Q\}$  are accordingly vectors of nodes structural displacements, potentials, external mechanical forces and charges coupled on the electrodes. Vector  $\{u\}$  gives all components of structural displacements of the actuator's discrete nodes for investigating trajectories of the contact point of actuator.

### Numerical investigation

Numerical study of piezoelectric actuator was performed to investigate vibration shapes and trajectories of contact point motion through the modal and harmonic response analysis. Finite element method was used for the simulation. Finite element model of the actuator was built with the following dimensions:  $L=0.05\text{m}$ ,  $H=0.003\text{m}$ . Total weight of the additional masses has varied from 5% till 50% of and beam weight. PZT-8 piezoceramics was used for simulation. Constant material damping was assumed in the model.

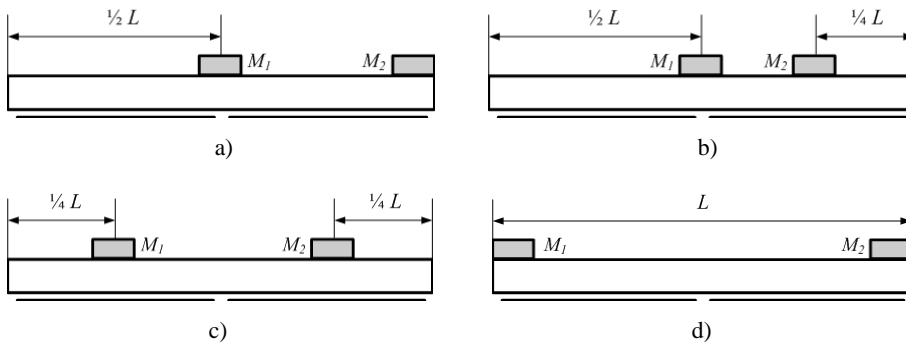


**Fig. 2.** The cases of additional masses location on the beam type actuator used for simulation

Four different locations of the masses on the beam top surface have been analyzed (Fig. 2). Locations have been chosen so that it coincides with node of longitudinal vibrations or location point has the maximum amplitude of vibrations. So two location cases are symmetric (Figs. 2a, 2b) and two are asymmetric (Figs. 2c, 2d). Modal analysis of piezoelectric actuator was done to find applicable modal shapes and natural frequencies of the actuator. Actuator has multimode vibration shapes due to the additional masses so dominating coefficients of the vibrations were applied to identify modal shapes with dominating longitudinal modes. Dominating coefficients are calculated as follows:

$$r_{jk}^n = \frac{S_j^n}{S_k^n}, \quad j \neq k \quad (9)$$

here

$$S_k^n = \sum_{i=1}^r (A_{ik}^n)^2, \quad r = \frac{l}{k} \quad (10)$$

where  $A_{ik}^n$  - vector of  $n$  modal shape,  $k$  and  $l$  – number of degrees of freedom in the node and in the model respectively. Physical interpretation of the dominating coefficients is the ratio between vibration energy components according to degrees of freedoms of the model. Modal shapes with the dominating 1<sup>st</sup> and 2<sup>nd</sup> longitudinal modes were investigated by analyzing coefficient  $r_{l2}$ , where indexes  $l, 2$  represent  $x$  and  $y$  direction of vibrations respectively (Fig. 1). Dependence of dominating coefficient  $r_{l2}$  from ratio of the additional masses and mass of the beam  $(M_1+M_2)/m$  are given in Fig. 3. It can be noticed that coefficient  $r_{l2}$  of the 1<sup>st</sup> longitudinal mode weakly depends on  $(M_1+M_2)/m$  ratio when cases of asymmetric location or masses is used (Fig. 3a). It means that modal shape remains unchanged when values of additional masses increases. In case of symmetric location of additional masses, the values of  $r_{l2}$  decrease when  $(M_1+M_2)/m$  ratio increases (Fig. 3a). It means that influence of the bending mode vibrations increases into modal shape of the actuator in these cases. Variation character of the coefficient  $r_{l2}$  doesn't depend on location case of the additional masses when 2<sup>nd</sup> longitudinal mode is used (Fig. 3b). In all cases  $r_{l2}$  values decrease when values of additional masses increases. Therefore it can be concluded that by varying values of additional masses and its location places, different ratio of the longitudinal and bending components of the multimode vibrations can be achieved.

The next step of investigation is to find dependences of parameters of the contact point motion trajectories from additional masses. Harmonic response analysis was performed for this task. Sinusoidal voltage was applied on electrodes of piezoceramic beam. Contact point is

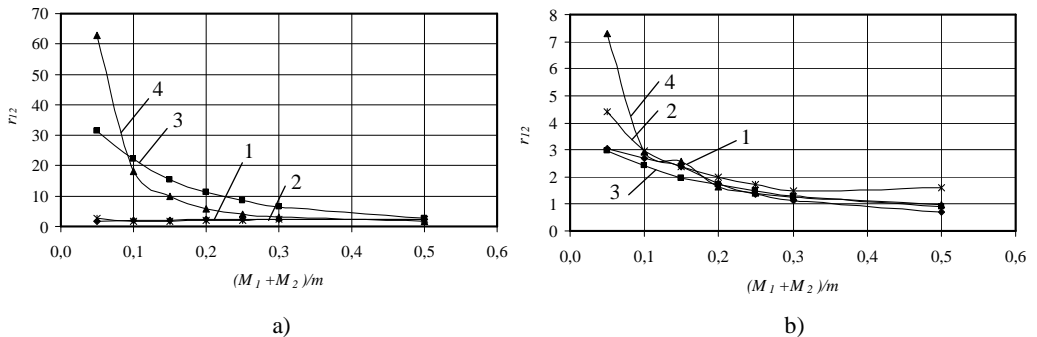


**Fig. 3.** Dependencies of dominating coefficient  $m_{l2}$  from ratio  $(M_1+M_2)/m$  calculated for: a) 1<sup>st</sup> and b) 2<sup>nd</sup> dominating longitudinal mode: 1 –  $(L/2 + L)$ , 2 –  $(L/2 + 3/4L)$ , 3 –  $(1/4L + 3/4L)$ , 4 –  $(0 + L)$

located at the top edge of the actuator's right side (Fig. 1). Two excitation schemes were used for simulations of the trajectories. The first scheme allows achieving direct motion and the second reverse motion of the slider. Principle of excitation schemes was described in Section 2. A 30V AC signal was applied to electrodes. Fig. 4 illustrates trajectories of the contact point's movement when values of  $(M_1+M_2)/m$  ratio is 0.1. By observing these trajectories it can be seen that trajectories of contact point has elliptical shape and directions of motion are opposite at different frequencies (Fig. 4). This means that slider will have direct and reverse motion when excitation at these frequencies will be applied. By comparing major semi axes of the ellipses it can be noticed that lengths of the axes are larger in Fig. 4b. It means that the contact point's motion and the strike, respectively, are more powerful at resonance frequency with 2<sup>nd</sup> dominating longitudinal mode. Rotation angle of the ellipses depends on excitation frequency and location of additional masses on the actuator as well.

Further investigation was carried out with the task to analyze the influence of additional masses to parameters of elliptical trajectories of the contact point. The length and rotation angle of major semi axis were analyzed when the ratio  $(M_1+M_2)/m$  varies from 0.05 till 0.5 while mass of the beam  $m$  remains constant. Multimode resonant frequencies with dominated 1<sup>st</sup> and 2<sup>nd</sup> longitudinal vibration modes were recalculated for each different values and location of additional masses. Results of calculations that are length and rotation angle of ellipses major axis are given in Figs. 5, 6 when different vibration modes are used. By observing graphs presented in Fig. 5 it can be noticed that the variation of the length of major semi axes strongly depends on location of the additional masses.

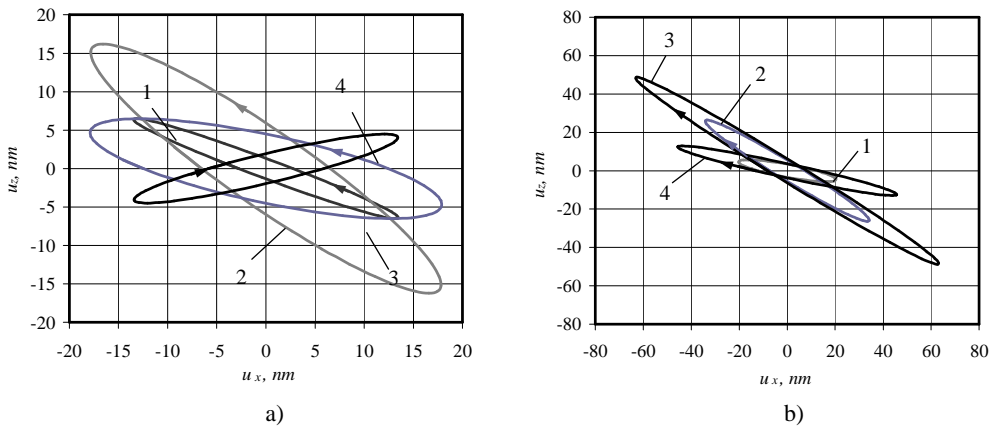


**Fig. 4.** Trajectories of the contact point motion when different locations of the masses are used: multimode vibrations with 1<sup>st</sup> (a) and 2<sup>nd</sup> (b) longitudinal dominating mode: 1 –  $(L/2 + L)$ , 2 –  $(L/2 + 3/4L)$ , 3 –  $(1/4L + 3/4L)$ , 4 –  $(0 + L)$

Graphs No. 1, 3, 4 (Fig. 5a) have similar character of variation and achieves highest value when ratio  $(M_1+M_2)/m$  value is equal to 0.5, while graph No. 2 nearly linearly decreases when weight of additional masses increases. This phenomenon can be explained so that vibration amplitudes increase due to decrement of damping in the system when total mass of the system increases. In case of graph No. 2 vibration amplitudes decreases due to location of the additional masses that suppress vibrations. Analyzing graphs shown in Fig. 5b it can be noticed that length of the ellipses major semi axis increases only in the case when masses are located at the nodes of the 2<sup>nd</sup> longitudinal mode. Length of semi axes decreases with increase of the ratio  $(M_1+M_2)/m$  in other cases because additional masses suppress 2<sup>nd</sup> longitudinal vibration mode.

Rotation angle of major semi axis of the ellipses presented as a function of ratio  $(M_1+M_2)/m$  in Fig.6. It must be indicated that rotation angle must have opposite sign in order to obtain proper stick during contact operation at 1<sup>st</sup> and 2<sup>nd</sup> longitudinal dominating frequency because direct and reverse motion must be obtained at these frequencies respectively. Fulfillment of this condition depends on ratio  $(M_1+M_2)/m$  and location of the masses. Analyzing graphs of rotation angle it can be noticed that graph No.2 (Fig. 6a) and graph No.3 weakly depends on ratio  $(M_1+M_2)/m$  because in these cases additional masses are located at the nodes of longitudinal vibrations of the beam and make small influence into vibrations. Other graphs in Fig. 6 have several peaks and this means that influence of components of longitudinal and

bending modes into multimode vibration changes depending on weight of additional masses by changing the angle of rotation.

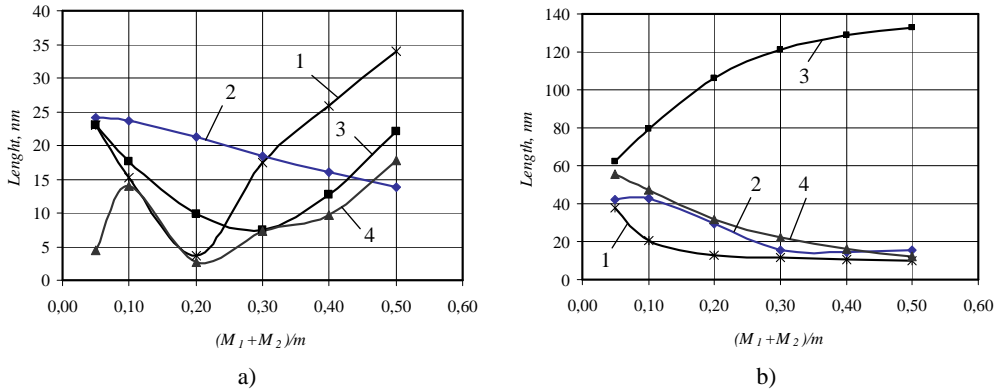


**Fig. 5.** Length of major semi axis of ellipses presented as a function of ratio  $(M_1+M_2)/m$ : a) – multimode vibrations with 1<sup>st</sup> longitudinal dominating mode, b) – multimode vibrations with 2<sup>nd</sup> longitudinal dominating mode: 1 –  $(L/2 + L)$ , 2 –  $(L/2 + 3/4L)$ , 3 –  $(1/4L + 3/4L)$ , 4 –  $(0 + L)$

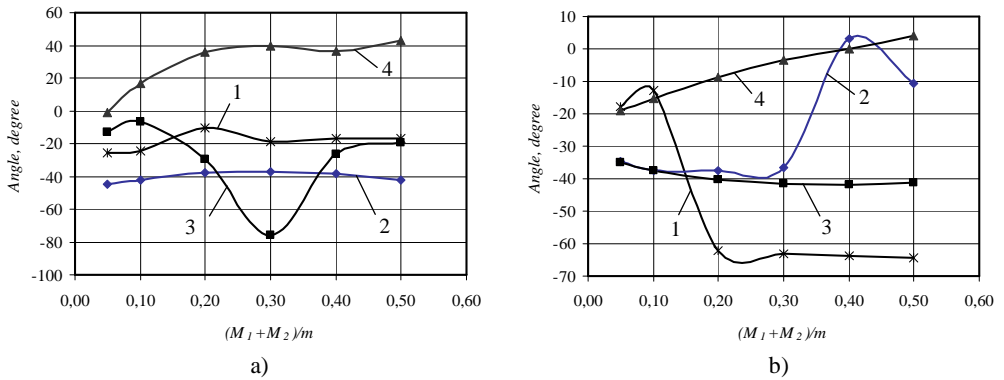


**Fig. 6.** Rotation angle of major semi axis of the ellipses presented as a function of ratio  $(M_1+M_2)/m$ : a) multimode vibrations with 1<sup>st</sup> longitudinal dominating mode, b) multimode vibrations with 2<sup>nd</sup> longitudinal dominating mode: 1 –  $(L/2 + L)$ , 2 –  $(L/2 + 3/4L)$ , 3 –  $(1/4L + 3/4L)$ , 4 –  $(0 + L)$

### Conclusions

Numerical model of piezoelectric actuator with two additional masses was developed and analyzed. It was shown that elliptical trajectories of contact point motion can be achieved applying different mass weight and different multimode resonant vibrations. Direct and reverse motion of the actuator can be obtained applying two different vibration modes. Length of major semi axis are larger when 2<sup>nd</sup> longitudinal dominating vibration mode is used so elliptical motion of contact point is more powerful at this mode. Length and rotation angle of major semi axis strongly depend on the weight and location of additional masses.

### Acknowledgement

This work has been supported by Lithuanian State Science and Studies Foundation, Project No. B-07017, “PiezoAdapt”, Contract No. K-B16/2009-1.

## References

- [1] **Uchino K., Giniewicz J.** (2003), *Micromechanics*, Marcel Dekker Inc., New York, p.504.
- [2] **Uchino K.** Piezoelectric ultrasonic motors: overview, *Journal of Smart Materials and Structures*, 1998, Vol.7, pp. 273-285.
- [3] **Bansevicius R., Barauskas R., Kulvietis G., Ragulskis K.** (1988), *Vibromotors for Precision Microrobots*, Hemisphere Publishing Corp., USA, p. 310.
- [4] **Sashida T., Kenjo T.** (1994), *An Introduction to Ultrasonic Motors*. Oxford Press, p. 235.
- [5] **Meirovitch L.** (1967), *Analytical Methods in Vibrations*, Prentice Hall, New York, p. 576.
- [6] **Filipov A.** (1970), Oscillations of deformable system, *Mashinostrojenije*, Moskva, p. 733 (in Russian).
- [7] **Gurgoze M.** On the Eigenfrequencies of Longitudinally Vibrating Rods Carrying a Tip Mass and Spring–Mass in-Span, *Journal of Sound and Vibration*, 1998, Vol. 216(2), pp. 295-308.
- [8] **Banerjee J. R., Sobey A. J.** Further Investigation Into Eigenfrequencies of a Two-part Beam–Mass system, *Journal of Sound and Vibration*, 2003, Vol. 265, pp. 899–908.
- [9] **Vasiljev P., Mažeika D., Kulvietis G.** Modelling and analysis of omni-directional piezoelectric actuator. *Journal of Sound and Vibration*, Vol. 308, Issue 3-5, Elsevier, 2007. p.867-878.